Hindawi
International Journal of Photoenergy
Volume 2019, Article ID 3452180, 13 pages
https://doi.org/10.1155/2019/3452180

Research Article

Confirmation of the Degradation of Single Junction Amorphous Silicon Modules (a-Si:H)

G. O. Osayemwenre and E. L. Meyer

Fort Hare Institute of Technology, University of Fort Hare, 1 Kings William Town Road, Alice 5700, South Africa

Correspondence should be addressed to G. O. Osayemwenre; gosayemwenre@ufh.ac.za

Received 4 June 2019; Revised 31 August 2019; Accepted 17 September 2019; Published 30 December 2019

Academic Editor: Huiqing Wen

Copyright © 2019 G. O. Osayemwenre and E. L. Meyer. This is an open access article distributed under the Creative Commons Attribution License, which permits unrestricted use, distribution, and reproduction in any medium, provided the original work is properly cited.

This study examines the degradation of single junction amorphous silicon (a-Si:H) photovoltaic (PV) modules. It summarises the main results obtained from over 7 years of field investigation of the degradation mechanisms of a-Si:H modules. The investigation was based on performance parameters such as fill factors, parasitic resistances, and ideality factors. The initial efficiencies for these modules were in accordance with the expected values; however, a significant decrease was observed during the monitoring period.

1. Introduction

The performance state of amorphous silicon (a-Si:H) solar modules after installation depends on the extent to which they have degraded over time. Performance assessment is an essential part of the photovoltaic (PV) module certification process. However, performance characterisation is required to be done a few minutes after outdoor deployment of the modules. The reason for such prompt characterisation is that manufacturers' ratings are often at variance with the actual performance of modules. Thus, initial assessments prior to the deployment of modules serve as baseline readings for future assessments. This initial assessment is necessary in view of the fact that the major problem that PV modules experience when exposed to environmental conditions is efficiency loss, which is the rationale for degradation analysis. Furthermore, when PV modules are deployed outdoors, thermal coupling and stress begin to set in after some time [1, 2], whereas the degradation of amorphous modules, which are known to be more prone to defects, starts within the first few hours of their deployment. This longer initial degradation time of a-Si:H creates room for the formation of a hot spot in the defective regions of the modules. This is unhealthy for the performance and reliability of PV modules. A high degradation of amorphous silicon solar modules has been recorded over time [3]. To overcome or reduce the degradation rate and increase the performance ratio, multijunction a-Si:H PV modules were introduced. Although multijunction a-Si:H modules have better performance and low initial degradation rates, their stability over a long period is still in question as a few studies have been done on their long-term monitoring especially in tropical (Africa) regions.

The place of degradation assessment in the quest to increase the performance of photovoltaic modules cannot be overemphasised. Several works have been done on this subject and the National Renewable Energy Laboratory (NREL) review is an example. The NREL's report on degradation of photovoltaic modules indicate that 78% of monocrystalline silicon solar modules (c-Si) experience about 1%/year degradation [4, 5]. Meanwhile, about 9% of thin film and amorphous silicon solar modules experience more than 4.1%/year degradation [4, 6]. However, the report also reveals that some a-Si:H modules experience decrease in their degradation rates and these appear in the form of negative degradations which show improvements. This can be linked to a recovery process for a-Si:H. The authors of the review admitted that there is need to update the data frequently since researchers exploit new technologies and production processes daily. Meanwhile, some of these production techniques slightly vary in terms of the expected standard procedures. The NREL's report is similar to that of Jahn *et al.* but their data slightly differ [6, 7]. It is important to note that

these reports are based on survey of literature rather than scientific sampling of experimental results [8]. As such, there is a possibility that modules with higher degradation rates could have been left out in the analyses [7–9]. According to Dirnberger *et al.*, long-term degradation rates of PV modules depend on the type of modules [10]. This implies that even though the degradation of double and triple junctions appear to be lower than that of single junctions, the long-term degradation rates depend on types of modules rather than on technology. This is why this study was birthed immediately as we observed that the initial degradation rate was slightly higher than what was expected. Adelstein *et al.* show a degradation rate that is more than 1%/year for dual junction a-Si:H modules [11–13]. However, the degradation rate of a triple junction was approximately 1% after a period of 6 years [13].

Though the performance of the a-Si module is prone to SW at the early stage, however, some other factors also affect their performance at long terms. Most of these factors are the results of degradation. These include temperature, series resistance, shunt resistance, cell cracking, soiling, and EVA degradation which affects reflections thereby contributing additional diffuse irradiance and shading of the module [13, 14]. Some of the aforementioned factors are subsequently discussed in this paper.

The PVPM 1001C module was used in the study for the outdoor characterisation. The accuracy of PVPM 1001C under a temperature range of -40°C to +120°C with an irradiance of 0-1300 W/m^2 is high [15–17]. The measuring accuracy of I-V is 1% for peak performance of +5%, provided the measuring time per scan is between 0.02 and 2 seconds (100 pairs of measurement value) [15, 18]. This is to prevent undesirable rise in temperature. Studies reveal [18, 19] that the performance of a PV module is inversely proportional to its rise in temperature. The knowledge acquired from such studies is necessary because the performance parameters like short-circuit current (I_{sc}), open circuit voltage (V_{oc}), fill factor (FF), and efficiency (Z) directly affect PV module performance [20, 21]. The increase in the temperature of PV modules can be caused by ambient environmental temperature changes, cloud patterns, and wind speed. While I_{sc} slightly increases, V_{oc} decreases with rising temperature. The performance of the PV module is less sensitive to temperature than irradiance changes but temperature changes are still significant [22–24]. In amorphous PV modules, performance output I-V curves are affected by light-induced degradation of modules. When an abnormal temperature rise occurs in an a-Si:H module, the fill factor decreases, the short-circuit current changes, and the open circuit voltage relatively remains unchanged [25–27].

The main aim of this study is to undertake both in-depth quantitative and qualitative analyses of the degradation of a-Si:H modules. To achieve this, an outdoor assessment of the modules which was necessary for the establishment of degradation was performed. Thereafter, an indoor assessment of the modules was done before undertaking a microelectrical analysis of the modules in two regions of interest. For the purpose of clarity and to avoid ambiguity in the use of terms, these regions of interest are termed "affected and nonaffected regions." Seven modules were used for this study, and they were numbered from 1 to 7. The module with the worst-case scenario was numbered 3. Therefore, module 3 is referred to as the "affected module" and others are referred to as the "nonaffected modules." Meanwhile, within the same modules, the areas where localised heating were predominant resulted in a higher surface heating of the regions; such regions are termed the "affected (defective) regions." This means that in module 3, the hot spot areas are referred to as the "affected regions." Nonetheless, a detailed explanation as to why module 3 is termed the worst performing module is subsequently presented in this study.

An infrared camera was used to map the surface temperature of the modules during the outdoor deployment; the detail of this process is reported in Osayemwenre *et al.* [28]. The infrared (IR) thermograph of the analysed temperature's profile indicates that the region without a hot spot has a maximum temperature of 27.5°C, while the temperature profile of the region with a hot spot was approximately 67°C. This may be due to a poor heat exchange in the defective region compared to the nondefective region. The high temperature gradient in the region is responsible for the thermal decomposition of the EVA material in this region [29] which resulted in the photothermal degradation shown in Figure 1.

2. Materials and Methods

It is extremely important to take an experimental look at degradation modes and mechanisms of a-Si:H modules so as to have a proper understanding of the PV module failure. This is necessary as it would enhance the comprehension of stability and durability of a-Si:H modules. Thus, degradation analysis of a-Si:H modules installed at the SolarWatt Park, the outdoor research centre of the Fort Hare Institute of Technology (FHIT), University of Fort Hare, Alice, is presented hereunder. Alice is on 32.787°S 26.834°E latitude and longitude, respectively, with an annual rainfall of about 386 mm during summer and a daily average maximum temperature range from 19°C in June to 31.6°C in February.

Outdoor performance characterisation I-V measurements of the modules were taken with a PVPM1001 IV tracer. The indoor characterisation was taken with a Keithley 4200 semiconductor characterisation system. In characterising the performance of the modules, their parasitic resistance which includes series resistance (R_s) and shunt resistance (R_{sh}) was calculated from measured values (data). These results are valuable parameters in degradation analysis; thus, particular attention was paid to the high R_s and low R_{sh} of module 3. The results include the first measurement taken on the 10th of April 2012 when the modules were first deployed outdoors. These results serve as baseline readings for future purpose. The second part of this study is the electrical characterisation of the modules using the Keithley 4200 IV tracer. This is an indoor assessment that was done before one of the modules was delaminated for microelectrical analysis using a four-probe I-V/C-V device. Table 1 presents the baseline characterisation of the seven a-Si:H modules used.

Figure 1: Single junction amorphous module (module 3) with insert of samples from the affected region (AS). AS stands for affected sample and sample from the nonaffected region (NS); NS stands for nonaffected sample while the arrows directly point to the position where they were taken from.

Table 1: Measured performance parameters of the seven modules investigated in this work. The corrected Standard Test Condition (STC) values are also listed for comparison.

	Measured					STC corrected	
Module	I_{sc} (A)	V_{oc} (V)	P_{max} (W)	FF (%)	η_{max} (%)	P_{STC} (W)	η_{STC} (%)
1	1.30	21.7	12.8	52.8	9.6	14.0	10.5
2	1.24	22.2	12.3	53.9	9.2	13.8	10.3
3	1.16	23.3	10.8	46.0	8.1	12.3	9.2
4	1.03	22.1	8.60	43.1	5.4	12.7	8.6
5	1.14	22.3	8.90	45.0	5.7	10.9	8.6
6	1.29	23.2	12.9	53.1	9.4	15.4	10.7
7	1.01	23.2	10.4	48.6	7.8	11.9	8.9
Average	1.17	22.6	11.0	48.9	8.0	12.7	9.5
% diff	18.01	5.15	32.81	20.04	43.75	29.71	30.58

These modules have the same dimensions, and they were produced by the same manufacturer. But the percentage difference between the highest value and the lowest value of each performance parameter, with respect to the average, is an indication that the manufacturing process and quality assurance of the modules are far from the required standard of PV modules. This anomaly is obvious in the corrected STC power which varies by as much as 29.7%. This variance would be unacceptable in an environment where quality is of utmost priority.

Equations (1) and (2) state the formula for correcting the measured maximum power and short-circuit current to STC values:

$$P_{STC} = \left[P_{max}\left(\frac{1000}{H}\right) + \gamma(T_{mod} - 25^{\circ}\mathrm{C})\right], \quad (1)$$

$$I_{STC} = \left[\frac{I_{SC} \times 1000}{H}\right] + (25 - T_{mod}) \times \alpha, \quad (2)$$

where P_{max} is the actual power measured under irradiance (H) at module temperature (T_{mod}) and t is the time duration. The temperature coefficient for power, $\gamma = 10.3$ mW/°C was obtained from Meyer's work [30]. This positive temperature coefficient is typical of a-Si:H modules. In order to have a clear picture of how the I_{sc} degrades with time, the measured I_{sc} was corrected to STC using equation (2) given above: where I_{sc} represents the measured short-circuit current, ISTC is the corrected STC I_{sc} values, T_{mod} is the measured temperature of the module, and α (A/°C) is the temperature coefficient for current.

3. Results and Discussion

3.1. Long-Term Degradation. The measurements from an outdoor module testing (OMT) taken from April 2013 to April 2017 were used for the long-term degradation analysis. Within these periods, especially 2013, 2014, and 2015, being the first four years of deployment, the modules were exposed to continuous outdoor solar irradiance. The long-term monitoring process commenced in 2013 which is a year after the initial deployment of the modules in 2012, and data were obtained accordingly. Thus, the long-term degradation analysis excludes the initial deployment period and measurements. The justification for excluding the measurements obtained within the first year of deployment from the long-term degradation analysis is to exclude the Staebler-Wronski effect (SWE). The SWE is the main degradation factor that occurs in a-Si:H during the first year of deployment, and it occurs as a result of the disordered nature of amorphous silicon (a-Si) solar cells [31, 32]. This degradation phenomenon is predominant during the first few months of outdoor deployment. Although SWE is indefinite, it accounts for about 18% of reductions in the efficiency of a-Si:H modules [33–36]. Furthermore, the exclusion of the first one-year initial measurement was important in order to account for the Staebler-Wronski effect (SWE). Therefore, long-term performance analysis entails only the period when the outputs of the modules were presumed to be stable after the short-term period.

3.2. I-V Characteristics. The *I-V* characteristics of the 7 modules were measured sequentially. This means that for each measurement, the meteorological conditions were slightly different. In order to have a fair comparison of the performance parameters of the 7 modules, the *I-V* characteristics were corrected for temperature and irradiance to the STC (1000 W/m^2 at 25°C) conditions. Out of the 7 modules, and for the sake of clarity, only results of the best performing module (module 6), the average performing module (module 4), and the worst performing module (module 3) are presented here. As at April 2013, module 3 had almost the same *I-V* characteristics with module 4; hence, their *I-V* overlapped, as seen in Figure 2(a). Figures 2(a) and 2(b) show the *I-V* characteristics of the aforementioned 3 modules, whose performance characteristics were obtained from the measurements that were taken in 2013 and repeated in 2017.

Figure 2 shows the *I-V* curves of the modules with the exclusion of module 5; some of the modules show similar performance, while Figure 3 compares the *I-V* curve of module 3 at different measurement times. It is crucial to reiterate that the *I-V* curves were corrected at STC. The correction was important in order to avoid the complexity of relying on data measured at 1000 W/m^2, as this is always a challenge in PV module characterisation [7].

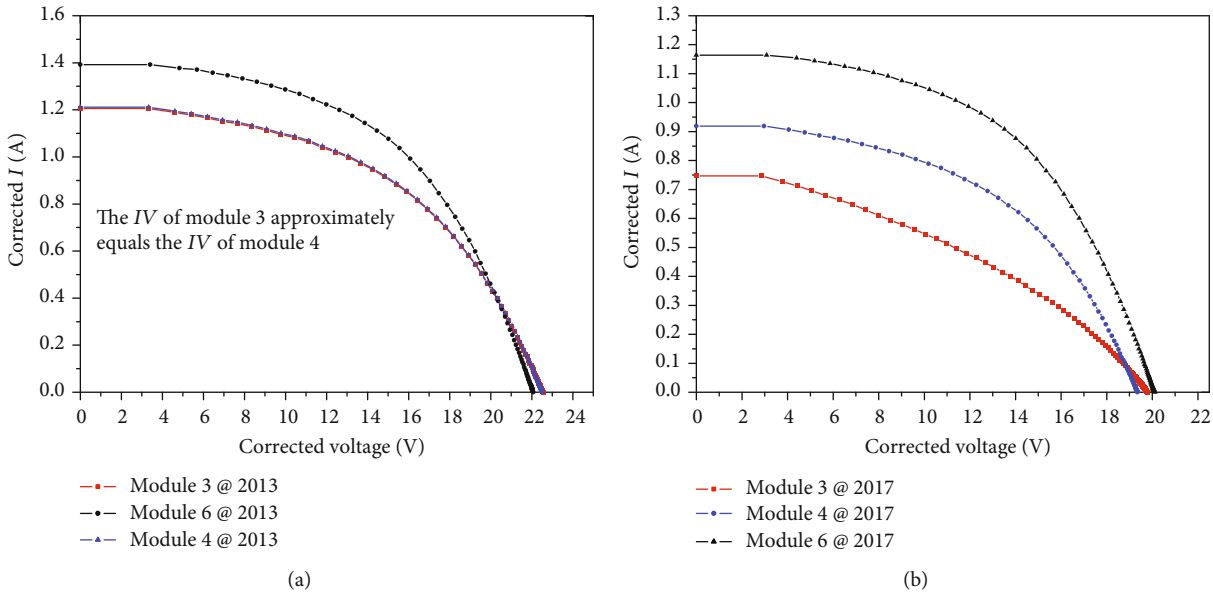

Figure 2: Corrected I-V characteristics of modules measured in the following years: (a) 2013 and (b) 2017.

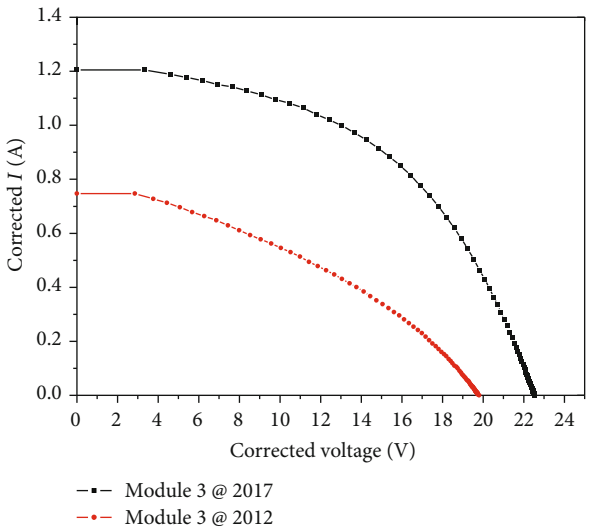

Figure 3: Single junction amorphous module I-V curves in the initial state (2013-04-20) and degraded state (2017-04-20) at noonday.

From the I-V characteristics presented in Figures 2(a) and 2(b), different performance parameters were obtained. The parameters obtained from Figure 2(a) are listed in Table 2, while the parameters extracted from Figure 2(b) are listed in Table 3. Table 4 presents the combined performance parameters of all the modules used in the study. Usually, the quality of a PV module is generally defined by its fill factor ($\mathrm{FF} = P_{\max}/I_{\mathrm{sc}}V_{\mathrm{oc}}$), [37]. As earlier shown, module 3 has the least FF. This means that module 3 had inferior quality as opposed to modules 4 and 6. In addition, the inverse of the gradient of the I-V curves at the point of $I = 0$ indicates series resistance (R_s). Hence, module 3 has the highest R_s followed by module 4, then module 6 which has the least. The purpose of comparing the FF and R_s of the 3 modules was to emphasise, firstly, that modules 3 and 6 are the least and best performing modules, respectively, among the three modules used as case studies. Secondly, that the higher value of the R_s obtained from module 3 may be responsible for its lower performance. Other parameters that are of paramount importance are the ideality factor, which can be inferred from the gradient of the logarithmic curve and the y-intercept, which gives a saturated current. The analysis of the ideality factor is presented in the later part of this paper.

3.3. Normalised I-V Characteristics. To compare the 3 modules (3, 4, and 6) in a single graph, the I-V characteristics of the modules were normalised. The normalised I-V curves of the three modules are presented in Figures 4 and 5. While Figure 4 presents the normalised I-V after the first few years of outdoor deployment, Figure 5 gives the normalised I-V of the modules in 2017. The normalised current of each module as a function of voltage assists in the performance analysis, for a proper comparison of the quality of the modules.

As early as 2013, module 3 started showing slight signs of mismatched cells. This is confirmed by the breakpoints in the curves. The I-V curve characteristics in Figure 4 show that module 3 had slightly mismatched cells in its series circuit connection [38–41]. However, the slope of each curve, judging from point $V = 0$, indicates a slight difference in their series resistance. The series resistance of modules 4 and 6 is similar but that of module 3 is higher by 29.9%. Figure 4 reveals some discrepancies in the performance parameters of the modules, and the series resistance is among the parameters that can be inferred from the normalised curve. At the point where $V = 0$, the slope of the curve shows variations in the series resistance as indicated by Tables 3 and 4. The nature of the slope of module 3 explains why its series resistance is more than those of the other

Table 2: Photovoltaic parameters of the three a-Si:H modules calculated from the measured data used for parameter characterisation analysis in April 2013.

Module	R_s	R_p	FF	I_{sc}	V_{oc}	P_{max}
3	9.7	280.5	44	1.20	22.26	9.9
4	7.6	462.0	51	1.22	22.27	13.7
6	6.8	401.9	59	1.38	22.09	15.1

Table 3: Photovoltaic parameters of the three a-Si:H modules calculated from the measured data used for the parameter characterisation analysis of April 2017.

Module	R_s	R_p	FF	I_{sc}	V_{oc}	P_{max}
3	24.5	156.5	34	0.75	19.72	6.9
4	19.6	264.9	41	1.00	19.34	11.4
6	16.5	305.6	54	1.14	20.71	14.2

Table 4: Photovoltaic parameters of the a-Si:H modules calculated from the measured data of the seven modules deployed on the outdoor module testing (OMT) system in April 2017.

Module	R_s	R_p	FF	I_{sc}	V_{oc}	P_{max}
1	21.4	233.0	47	0.90	23.73	10.2
2	**19.6**	**264.9**	**51**	**1.00**	**23.48**	**12.4**
3	24.5	156.5	34	0.75	19.72	6.9
4	19.6	264.9	41	1.00	19.34	11.4
5	18.5	234.8	54	0.96	23.10	12.4
6	16.5	305.6	54	1.14	20.71	14.2
7	**18.5**	**334.8**	**54**	**1.21**	**24.10**	**14.4**

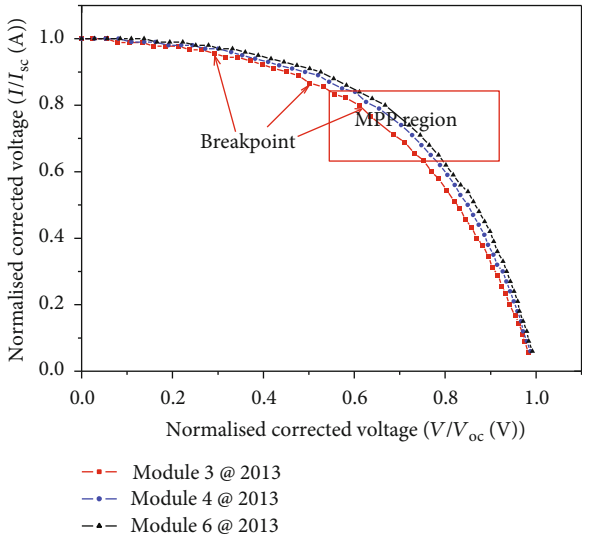

Figure 4: Normalised I-V characteristics of the a-Si:H modules (3, 4, & 6) in 2013.

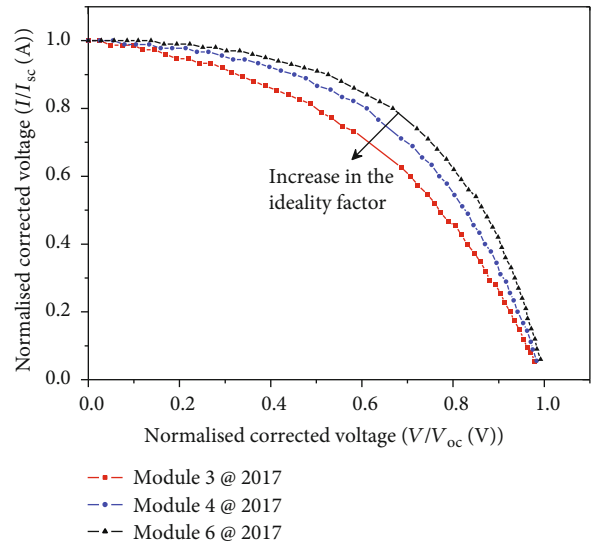

Figure 5: Normalised I-V characteristics of the a-Si:H modules (3, 4, & 6) in 2017.

modules. The other parameter that can be inferred from the I-V curve is the ideality factor. The ideality factor of a module reflects on the shape of the normalised I-V curve. The degree of flattening of the normalised I-V curve at the point of the maximum power point (MPP) indicates the magnitude of the ideality factor as seen from the red box. In Figure 4, modules 6 and 4 show an almost identical ideality factor, while module 3 shows a bit of a different ideality factor from the other modules. The normalised I-V curve of the modules after four years is presented in Figure 5, and the results seem quite different from what was observed in Figure 4.

For the normalised I-V characteristics of the three modules, each current was normalised to I_{sc} and the voltage to V_{oc}. The curve indicates that module 6 has the least series resistance and module 3 has the highest among the three modules. In the same order, module 6 has the highest shunt resistance, while module 3 has the lowest shunt resistance. The normalised I-V as demonstrated in Figure 5 shows that the ideality factor of the modules degraded significantly after 5 years. Module 3 experienced the highest reduction in its ideality factor due to the degrading ideality factor and an increase in the leakage current. The implication of this is that module 3 experienced an increase in its dangling bond density, as well as an increase in its leakage current compared to others. Furthermore, as the defect density increased, the series resistance also increased. This is occasioned by the rise in the series resistance of the material and as a result of the increase in the recombination current.

To enhance understanding, it is important to examine a diode which is the smallest building block of every PV module. Hence, from the diode's equation, also known as Shockley's equation presented in equation (5), it is possible to explain the behaviour of PV modules [42]. I_0 stands for the reverse saturation current. The performance of PV cells can be estimated from the ideality factors which indicate

the extent of deviation from the ideal diode characteristics. From the results present herein, n ranges from 1 to 7 and theoretically, as the value of n rises, the forward diode current decreases. This correlates with the results presented in this study. The value of the diode current is a function of the I_0 as well as n for a given bias voltage. It is also crucial to note that the shunt resistance in an a-Si:H module turns negative once there is an increase in the reverse bias voltage during movement from the p-layer to the n-layer. Performance enhancement in a p-i-n PV cell correlates to changes in the defect density of states in interface regions [43]. Therefore, decrease in the performance of module 3 is believed to be mainly due to an increase in the defect density of the i-n interface region after degradation. Furthermore, increase in defect density is due to temperature dependence of dangling bonds in p-i-n solar cells. This is because more dangling bonds are formed at a higher temperature. The reason why more of these occurred in module 3 and not in other modules is because of the localised heating which resulted from excessive hot spot formation.

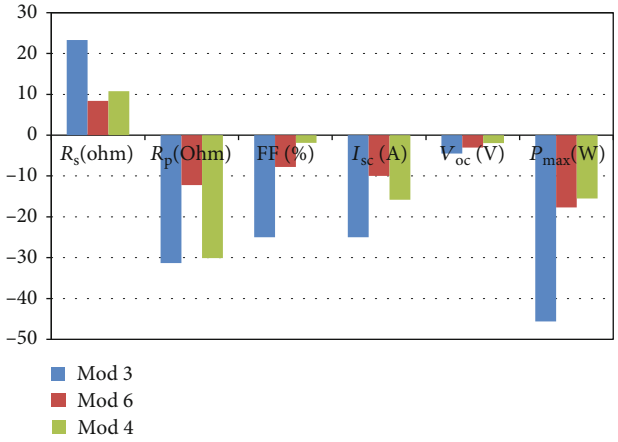

Figure 6: Percentage change from 2013 to 2017 in various performance parameters of the I-V curve components: short-circuit current (I_{sc}), open circuit voltage (V_{oc}), fill factor (FF), shunt resistance (R_{sh}), series resistance (R_s) and maximum power (P_{max}) for modules 3, 4, and 6.

3.4. Degradation of Individual Performance Components. In order to understand the factors responsible for the degradation of various performance parameters, the observed degradation of the three modules, out of the seven modules from the outdoor testing measurements, is studied. These parameters are divided into two categories. The first category is those used for the performance assessment known as performance parameters and they include I_{sc}, V_{oc}, FF, and P_{max}. The second category is those parameters used for accessing the degradation and they include R_s and R_{sh}. Figure 6 shows the percentage degradation (% change) of the I-V component, based on the result at which the annual degradation rate was calculated.

Shunt and series resistance were calculated in order to identify the contribution of these parameters to the degradation suffered by the modules. The interest here is to profess an explanation for the degradation of the V_{oc} and I_{sc} observed in this study. The computer simulation work of Stuckelberger *et al.* [44] shows that an increase in carrier concentration, in the order of $10^{19}\,\text{cm}^{-3}$ to $10^{20}\,\text{cm}^{-3}$ in a p-layer, can result to a rise in the value of V_{oc}. Wronski's latest work from a light-induced degradation (LID) shows that an increase in the defect density in the intrinsic layer of an a-Si:H leads to a decrease in the value of V_{oc} [45, 46]. This was confirmed by the work of Aste *et al.* when they intentionally introduced defects in a module and observed an increase in the value of V_{oc} [45]. This study observed degradation in the value of V_{oc} which resulted from photothermal degradation as explained by Osayemwenre *et al.* [47]. This photothermal degradation is known to be prone to interchemical diffusion [47, 48], and it leads to a rise in the defect density in the interstitial layers. Consequently, there is a possible increase in the impurity level, leading to a rise in the defect density in the intrinsic layer of this module under investigation. Therefore, one can conclude that this decrease in V_{oc} is due to a rise in the defect density inside the intrinsic (i-Si) region. The decrease in V_{oc} is also related to the state of the p-i-n junction diode. Therefore, any occurrence of defect which can damage the p-i-n structure can affect the value of V_{oc}.

The annual P_{max} degradation of a-Si:H used in this work varies from module to module. For the best performing module, the annual P_{max} degradation is less than -2.6% per year and this is far more than -0.8% per year for monocrystalline Si modules [49]. The highest P_{max} degradation previously recorded is -2% per year, and this falls within the range of the recent reports [50]. Thus, the difference in the result of this study may be because the former authors used an irradiance of 900 W/m^2 and difference in PV module technology. The degradation rate of -2.6% per year makes it seem impossible for these modules to meet the 20-25 years P_{max} warranty known for PV modules. This could be the reason why some a-Si:H manufacturers do not promise a warranty, as reported by Duke *et al.* with regard to the Kenya PV market [51]. The high degradation rate is also linked to the absence of a bypass diode. The degradation of module 4 was -2.95% per year; it was slightly higher than that of module 6, and this is understandable since the module has a different performance. The least performing module had the highest degradation rate of -7.9% per year; hence, further analysis is made with reference to this module because of its degradation rate.

3.5. Degradation Explained. To understand the degradation of the amorphous silicon module, there is need to study both the performance parameters (I_{sc}, V_{oc}, P_{max}, and η) and the quality assessment parameters (FF, R_s, and R_{sh}). Module parameters are the key factors required to establish the quality, performance, and reliability of PV modules [51, 52]. The V_{oc} of a-Si:H is very sensitive to a rise in temperature and also depends on the quality of its p-i-n diode. This is well explained by

$$V_{oc} = \frac{E_g}{q} - \frac{nkT}{q}\left(\ln \frac{I_{0\,max}}{I_{sc}}\right), \tag{3}$$

where E_g is the energy band gap and $I_{0\,\max}$ is the maximum reverse saturation current, while the fill factor is calculated from the following equation [52]:

$$\mathrm{FF} = \frac{P_{\max}}{V_{oc} \times I_{sc}} = \frac{V_{\max} \times I_{\max}}{V_{oc} \times I_{sc}}. \quad (4)$$

Current is the most used parameter of PV cells and modules when characterising performance [22]. For a degraded a-Si:H, the equation of the double diode model is preferred and this is given by

$$I = I_0 \left[\exp\left(\frac{q(V - IR_s)}{nkT}\right) - 1\right] + \left(V - \frac{IR_s}{R_{sh}}\right) - I_L, \quad (5)$$

where I_0, q, n, k, T, R_s, R_{sh}, and I_L stand for reverse saturation current, electron charge, ideality factor, Boltzmann constant, temperature, series resistance, shunt resistance, and light generated current, respectively [53, 54]. While the efficiency of Si solar cells is defined by equation (6), the relationship between efficiency and temperature is defined by equation (5).

$$\eta = \frac{P_{\max}}{P_{in}} = \frac{V_{\max} \times I_{\max}}{E \times A} = \frac{FF \times V_{oc} \times I_{sc}}{E \times A}, \quad (6)$$

$$\eta_c = \eta_{\mathrm{Tref}}[1 - \beta_0(T_c - T_{\mathrm{ref}})]. \quad (7)$$

Here, $\eta_c$andη_{Tref} are the efficiencies at room temperature and module operating temperature, respectively; β_0 is the temperature coefficient, which is $0.004\,\mathrm{K}^{-1}$ [54]. T_c and T_{ref} are the cell and reference temperatures, respectively [25, 54]. P_{in} and $P_{\max}$ are the maximum power input and power output, respectively, A is the aperture area of the module, and E is the irradiance.

In this study, the seven modules that were studied showed signs of hot spot formations, but module 3 exhibited the highest hot spot formation with temperature of up to 65°C observed at the hot spot region [28, 55]. In addition, there was a significant decrease in the short-circuit current of each module after some years. The decrease was more than the 1% per year that was expected [56–58]. While the open circuit voltage decreased slightly, the fill factor also showed some significant degree of decrease, but the decrease of V_{oc} and FF was not commensurate with the I_{sc} decrease. Although for module 3, the I_{sc} and FF showed the highest decrease, the decrease of its V_{oc} was not as high as that of module 4.

3.6. Degradation of Short-Circuit Current (I_{sc}). To remove soiling, all the modules were cleansed daily before measurements were taken. The step above was taken because soiling usually contributes to the degradation of I_{sc} by reducing the quantity of the irradiance that reaches the front layer of the modules. However, the other parameters are not affected by soiling, but it can influence some factors which can reduce the I_{sc} and greatly affect the performance of the modules [59, 60]. One of such factors is EVA discoloration of module encapsulant. This affects the quantity of short wavelength photons that can be transmitted [30, 31, 61]. At the end of the monitoring period, module 6 lost 10% of its I_{sc} value, module 4 lost 15.8%, and the worst performing module lost 25% of its I_{sc}. These translated into an annual degradation of -1.9%/year, -2.7%/year, and -4.2%/year for module 6, module 4, and module 3, respectively. Again, these values surpass the -1%/year expected for a-Si:H PV modules when deployed outdoors [61, 62].

3.7. Degradation of Open Circuit Voltage (V_{oc}). As identified earlier in Section 3.4, each module experienced a significant level of V_{oc} degradation, but the amount of V_{oc} decrease varied from one module to another. The possible explanation for the decrease in V_{oc} can be linked to the quality of the diode of the modules, which, in this case, is the p-i-n [63, 64]. The deterioration of the quality of the p-i-n junction of the module is the main cause of V_{oc} degradation, and this can also result in an increase in saturated current. Hence, one will expect an ideality factor that is greater than 1 [65]. In some instances, the poor quality of diodes can lead to a rise in the saturated current or ideality factor that is greater than one [66]. Meanwhile, further investigation is needed to explain the quality of the a-Si:H diode (p-i-n). In addition, the high level of decrease in V_{oc} is due to the long period of exposure, since defect density increases with time. Lastly, the fall in the value of V_{oc} can also be partially attributed to the Staebler-Wronski effect (SWE) [67, 68]. The time within which the SWE can be said to be totally inactive is still under controversy because there are no consensus assertions regarding its mechanism [69–71]. But what is sacrosanct is that the SWE is fully active during the early stages of the deployment of a-Si:H modules, and as exposure time increases, the SWE drastically decreases.

3.8. Degradation of Fill Factor (FF). The results of the seven a-Si:H modules presented showed a significant variation in their fill factors. From this, it can be assumed that the series and shunt resistance of the modules had a significant contribution to the observed degradation. The degradation observed in the a-Si:H modules used in the study is due to the decrease experienced from their fill factors. This fill factor degradation is due to the net effect of both the parasitic resistance and open circuit voltage ($\mathrm{FF} = P_{\max}/I_{sc}V_{oc}$). The parasitic resistance effect can be due to an increase in the series resistance and a decrease in shunt resistance or either of them. In some cases, it may be due to an increase in the series resistance or decrease in the shunt resistance as observed in the study. There was also no obvious electrical connector degradation except in module 3. This is evident in Figure 1, which shows a complete decay of the connector and some degree of decay in module 4, which is not shown.

3.9. Performance Assessment. In order to validate the previous outdoor measurements, an indoor electrical characterisation was done using the solar simulator as the light source. It is crucial to note that the indoor electrical measurements were done approximately five years after the modules were deployed outdoors. One major observation from the indoor measurements is the difference in the values of the V_{oc} of

all the modules. The indoor value of the V_{oc} is seen to be higher than what is obtainable from a PVPM outdoor characterisation. This could be due to the low temporal stability in the new solar simulator currently installed at the SolarWatt Park of FHIT. Two kinds of measurements were done using a Keithley IV 4200 SCS, namely, light I-V and dark I-V measurements. The light I-V and dark I-V measurements are presented in Section 3.11.

Another parameter that is of utmost importance to degradation analysis is the P_{max}. To determine the output of each module, the maximum power at STC was calculated from the measured I-V curves. The results are presented in Figure 7. The outdoor measurements presented above showed a V_{oc} depreciation as high as 4.8%, while the lowest was 1.9%. But from the indoor characterisation, the highest reduction was 1.3% and the lowest was 0.9%, and these results fall within the range of the degradation expected for a-Si:H modules. The reduction is mainly due to the metastable effect, which enables the temporary recovery in the absence of continuous sun light and other environmental factors that are capable of influencing defect density. Figure 7 shows the combined P_{max}, vs. voltage curves of all the modules, with module 3 showing the worst performance judging from the P_{max}.

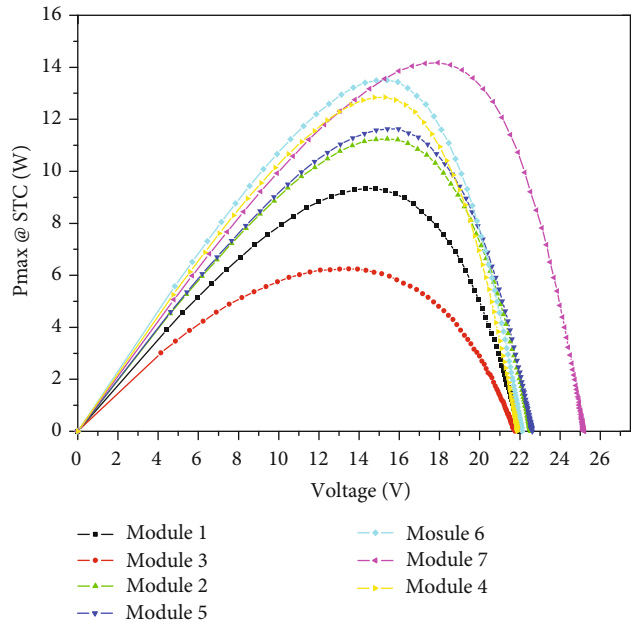

Figure 7: The power-voltage characteristics of a-Si:H of the 7 modules.

3.10. Justification of the Observed Degradation. In amorphous silicon modules, degradations are linked to the quasistable behaviour under the sun; this is known as the Staebler-Wronski Effect. This is why a long-time analysis is the best method to establish degradation in a-Si:H. These monolithic fabricated modules under investigation have no external bypass diodes for protection against shading. More so, due to the fabrication techniques used for the a-Si:H, even a bargaining shade on the edge of the module can encourage hot spot formation, thus leading to the reverse bias of the cells in such a region. A small shaded region of the module can also result in a significant reverse bias stress; such shading can result from the accumulation of dirt on the frame edge of the module. The setup of the module is done in such a way that all the cells are symmetrical with the frame edges. Hence, as the exposure time increases, the formation of hot spot increases in certain regions, leading to induced degradation which results from the reverse biased nature of the cells in the hot spot centre. The vertical tilting of the cells can encourage the accumulation of dust at the lower part of the frame edge; hence, without protection, this results in huge reverse biased cells because the a-Si:H is very susceptible to reverse bias. This is clear from the photo image of module 3 showing the region of complete damage and photothermal degradation in some parts of the module. Figure 1 shows EVA discoloration and cracks resulting from thermal stress and the region where photothermal degradation occurred. This cannot be said to be the sole cause of the degradation observed; the manufacturers' constructions and designs of the module are also contributing factors.

3.11. Leakage Current and I-V Characteristics. The dark I-V measured with a semiconductor characterisation system (4200 SCS) or Keithley did not reveal much abnormality in the I-V curves. This is primarily because carrier charges were not excited during the measurements. The I-V did not show much deviation from the normal I-V curve of a-Si:H modules, since module I-V depends on the number of defective cells present. Here, two modules were characterised with the semiconductor characterisation system (4200 SCS), and these modules are module 3 (affected module) and module 4 (nonaffected module). The results of the dark I-V characteristics for the measurement of the modules are shown in Figure 8. It is obvious that all the cells in the nonaffected module are in perfect states as the voltage increased above 15 V. However, in terms of stability and the transportation modes of the carrier mechanism which occur in each module, it is not enough to understand the state of the modules by merely looking at the curves. Hence, a semilog I-V of the module is required; with that, one is able to understand the predominant mechanism of the transportation and the state of the p-i-n junction.

The results of the semilog I-V characteristics for the measured for the 3 modules are shown in Figures 9–11. These figures represent the semilog I-V characteristics for 3 modules previously investigated in Section 3.3. As the voltage increases above 15 V, it became obvious that not all the cells in the nonaffected modules are in perfect states. Thus, from the curve, the saturation current and the ideality factor of each curve were obtained and calculated based on the theory governing the equations defined below:

$$\ln(I) = \ln(I_{ss}) + \frac{qV}{nkT}, \qquad n = \frac{q}{kT}\frac{dV}{d\ln(I)}. \tag{8}$$

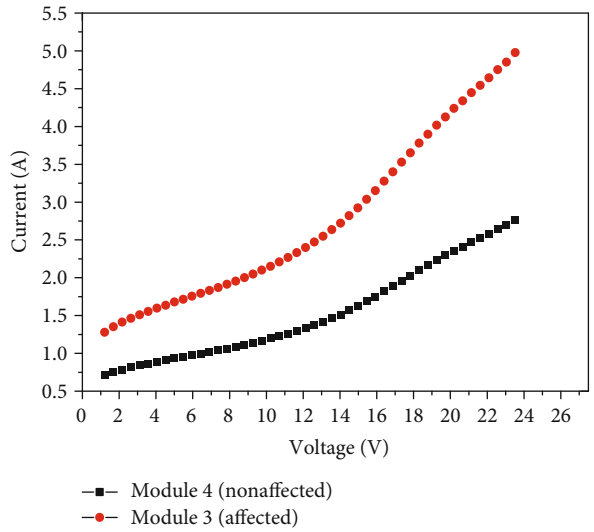

Figure 8: The figure presents the dark I-V curve of both the affected module (black curve) and the nonaffected module (red curve).

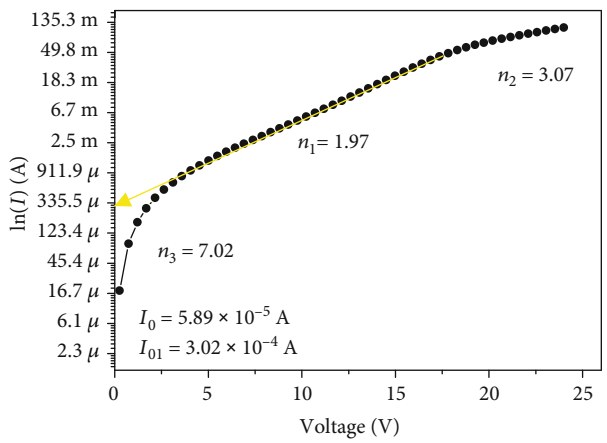

Figure 9: The figure presents ln (I) vs. V for 29 cells of the a-Si:H in the affected module 3.

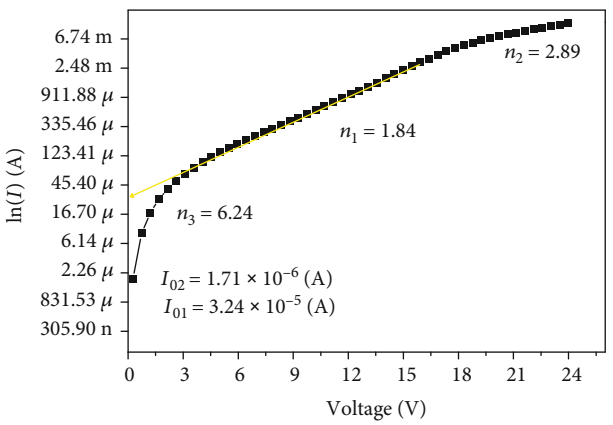

Figure 10: The figure presents ln (I) vs. V for 29 cells of the a-Si:H in module 4.

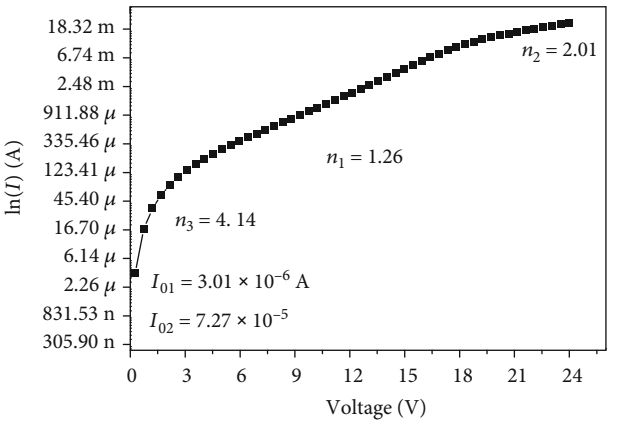

Figure 11: The figure presents ln (I) vs. V for 29 cells of the nonaffected module (module 6).

The ideality factor gives an indication about the stability and degree of leakage of the carriers. The affected module is presented in Figure 9, with an n value of about 2 in the straight region of the curve and n about 7 at a low applied voltage. The semilog I-V characteristics of modules 4 and 6 are presented in Figures 10 and 11, respectively.

The n_1, n_2, and n_3 of the nonaffected module are quite low compared to those of the affected module, although its n is a little more than one expected of PV modules. This is understandable considering that each module showed some degree of degradation that is more than the values that the literature predicted for PV modules from previous analysis.

4. Discussion

When the I-V is plotted in a logarithmic scale, the resulting curve could be divided into three parts, and each part connotes a different quality of a module. This explanation is different from Sidawi *et al.'s* work where the authors presented only two parts of the curve [72]; here, the three parts are clearly seen. For the sake of easy comprehension, part two is first presented. The second part begins from 4 V to approximately 15 V which is close to the compliance voltage. This part is very important since the slope of the curve is determined by it. It is also important to note that the extrapolation of this region gives a vertical intercept which is equal to the saturated current. The first part (part 1) begins from 0 V to 4 V; based on the manufacturer definition, this is outside the compliance voltage and this region relates to leakage current within the module. Part I regions indicate the presence of defects in the module, even at low voltage; hence, the leakage current is formed because of the presence of a hot spot in this region of the module. This is in accordance with Sidawi *et al.'s* previous observation of leakage current in part 1. This also relates to the recombination current within the module. The presence of a hot spot is believed to create weak regions in PV modules; this forces the electrons to flow in the reserve path of the p-i-n junction [40, 72]. The third region of the semilog I-V curve extends from 15 V to 25 V, which is the range of a nominal operation voltage, and this region is associated with a high

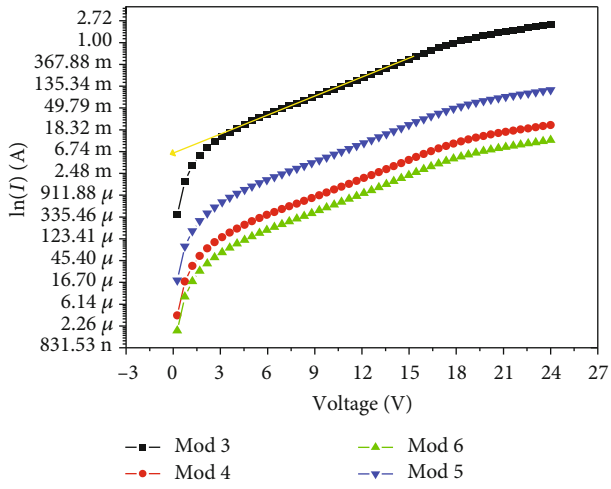

Figure 12: The figure presents ln (I) vs. V of all 4 modules.

voltage. In Figure 12, the combined semilog I-V is presented; the semilog of the short current I_{sc} was extracted from the respective figures.

The saturation current required for this calculation was obtained by extrapolating the semilog I-V curve. There are two types of saturated current associated with a degraded a-Si:H. As explained from the double diode model, they are I_{01} from the first part of the equation and I_{02} from the second part of the double model equation. I_{02} is extrapolated from the vertical intercept while I_0 is obtained from the linear part of the ln (I) vs. V curves as indicated by the yellow line in Figures 9, 10, and 12. The nature of the ln (I) curves shows that thermionic emission is the main transportation mode in these measurements [53]. However, the changes in n at a lower voltage indicate that other transportation modes may be present in moderate levels. As the contributions of the other modes of carrier transport increase, the value of n at a lower voltage also increases. This is obvious in the affected module where $n > 7$; this means a higher degree of recombination current. This connotes the defective diode inside the space charge region of the module. The most significant of these transport modes, as seen in Table 1, is the decrease in the shunt resistance of module 3; this resulted in excessive leakage current through the broken junction. There appears to be fewer alterations in the straight-line region of the curve where the slope is calculated. This is because the curve is for a whole module of 29 cells, whereas the defective cells have less contribution to the sink current.

5. Conclusion

In this study, the effect of degradation on the performance parameters of a-Si:H solar modules is reported. The study involves both outdoor and indoor characterisations of a-Si:H. While the outdoor measurements were used to analyse the long-term degradation of the modules, the indoor measurements were used to investigate the rectifying properties in terms of leakage current. The study established that low shunt resistance is a major contributing factor to the degradation of a-Si:H modules, as this creates room for an increase in the leakage current, as depicted in the double exponential equivalent circuit model. This study also reveals that a lot of factors need to be considered for a proper interpretation of degradation mechanisms. The percentage degradation of each parameter from the modules studied reveals that module 6 is closer to the value reported in the literature, which is 1%/year for V_{oc} and 2%/year for I_{sc}, while the worst-case scenario module shows a higher degradation. The semilog I-V is a power tool for analysing the diode quality and the state of the p-i-n junction. More so, for the a-Si:H modules, three parts in the ln (I) vs. V were observed, and each region of the curves showed a different ideality (n) value. The most degraded module showed a lower shunt resistance or higher shunt path and, at the same time, very low potential height, which indicates that other modes of transportation of carriers can easily occur in a module like module 3.

Data Availability

The data used to support the findings of this study are included within the article.

Conflicts of Interest

The authors declare no conflict of interest.

Acknowledgments

The authors would like to express their gratitude to the following organizations: the Govan Mbeki Research and Development Centre at the University of Fort Hare, the National Research Foundation, and the Department of Science and Technology (PV spoke).

References

[1] W. Herrmann, M. Adrian, W. Wiesner, and T. Rheinland, "Operational behaviour of commercial solar cells under reverse biased conditions," in *Proceedings of the Second World Conference on Photovoltaic Solar Energy Conversion*, pp. 2357–2359, 1998.

[2] G. Kleiss, K. Bucher, P. Ragot, and M. Chantant, "Monitoring outdoor performance and photodegradation of a-Si:H modules by evaluation of continuously measured IV curves," in *Proceedings of 1994 IEEE 1st World Conference on Photovoltaic Energy Conversion-WCPEC (A Joint Conference of PVSC, PVSEC and PSEC)*, vol. 1, pp. 531–534, IEEE, December 1994.

[3] S. B. Darling, F. You, T. Veselka, and A. Velosa, "Assumptions and the levelized cost of energy for photovoltaics," *Energy & Environmental Science*, vol. 4, no. 9, p. 3133, 2011.

[4] D. C. Jordan and S. R. Kurtz, "Photovoltaic degradation rates—an analytical review," *Progress in photovoltaics: Research and Applications*, vol. 21, no. 1, pp. 12–29, 2013.

[5] D. C. Jordan and S. R. Kurtz, "Thin-film reliability trends toward improved stability," in *Proceedings of the 37th PV Specialists Conference*, Seattle, WA, USA, 2011.

[6] U. Jahn and W. Nasse, "Analysis of long-term performance and reliability of PV systems," *IEA-PVPS Task 2 Report*, PVPS Annual Report 2003 - IEA-PVPS, 2003.

[7] K. Branker, M. J. M. Pathak, and J. M. Pearce, "A review of solar photovoltaic levelized cost of electricity," *Renewable and sustainable energy reviews*, vol. 15, no. 9, pp. 4470–4482, 2011.

[8] J. H. Wohlgemuth and B. P. Solar, "Long term photovoltaic module reliability," *NCPV and solar program review meeting*, pp. 179–183, 2003.

[9] S. M. Pietruszko, B. Fetlinski, and M. Bialecki, "Analysis of the performance of grid connected photovoltaic system," in *2009 34th IEEE Photovoltaic Specialists Conference (PVSC)*, pp. 48–51, Philadelphia, PA, USA, 2009.

[10] D. Dirnberger, W. Heydenreich, and K. Kiefer, "Performance of thin film PV technologies—Fraunhofer ISE experience form field and laboratory measurements," in *6th International Thin Film Conference*, Würzburg, Germany, February 2010.

[11] J. Adelstein and W. Sekulic, "Performance and reliability of a 1-kW amorphous silicon photovoltaic roofing system," in *Proceedings of the 31st PV Specialists Conference*, pp. 1627–1630, Lake Buena Vista, FL, USA, 2005.

[12] P. McNutt, J. Adelstein, and W. Sekulic, *Performance evaluation of a 1.5-kWdc a-Si PV array using the PVUSA power rating method at NREL's outdoor test facility (no. NREL/CP-520-38971)*, National Renewable Energy Lab.(NREL), Golden, CO (United States), 2005.

[13] J. Adelstein and W. Sekulic, *Small PV systems performance evaluation at NREL's outdoor test facility using the PVUSA power rating method (No. NREL/CP-520-39135)*, National Renewable Energy Lab.(NREL), Golden, CO (United States), 2005.

[14] IEC 60904-3, *Photovoltaic devices - Part 3: Measurement principles for terrestrial photovoltaic (PV) solar devices with reference spectral irradiance data*, 3 edition, 2016.

[15] A. Wagner, "Peak-power and internal series resistance measurement under natural ambient conditions," in *Proceedings EuroSun*, vol. 5, June 2000.

[16] C. Bendel and A. Wagner, "Photovoltaic measurement relevant to the energy yield," in *3rd World Conference onPhotovoltaic Energy Conversion, 2003*, vol. 3, pp. 2227–2230, IEEE, May 2003.

[17] C. Bendel and A. Wagner, "Photovoltaic measurement relevant to the energy yield," in *WCPEC-3, World Conference on Photovoltaic Energy Conversion*, pp. 1–4, Osaka, Japan, 2003, Pr. No 7P-B3-09.

[18] K. M. Schulte and A. Wagner, "Die effektive solarzellenkennlinie.-Anwendung in der teillast-berechnung," in *Proceedings*, vol. 17, 2002.

[19] A. Gregg, R. Blieden, A. Chang, and H. Ng, "Performance analysis of large scale, amorphous silicon, photovoltaic power systems," in *Conference Record of the Thirty-first IEEE Photovoltaic Specialists Conference, 2005*, pp. 1615–1618, IEEE, Lake Buena Vista, FL, USA, January 2005.

[20] S. M. Sze, *Physics of semiconductor devices*, John Wiley & Sons, New York, 1981.

[21] G. Landis, R. Rafaelle, and D. Merritt, "High temperature solar cell development," in *19th European Photovoltaic Science and Engineering Conference*, Paris, France, June 2004.

[22] J. J. Wysocki and P. Rappaport, "Effect of temperature on photovoltaic solar energy conversion," *Journal of Applied Physics*, vol. 31, no. 3, pp. 571–578, 1960.

[23] J. C. C. Fan, "Theoretical temperature dependence of solar cell parameters," *Solar Cells*, vol. 17, no. 2-3, pp. 309–315, 1986.

[24] P. Singh, S. Singh, M. Lal, and M. Husain, "Temperature dependence of *I–V* characteristics and performance parameters of silicon solar cell," *Solar Energy Materials and Solar Cells*, vol. 92, no. 12, pp. 1611–1616, 2008.

[25] D. J. Friedman, "Modeling of tandem cell temperature coefficients," in *25th IEEE Photovoltaic Specialists Conference*, pp. 89–92, IEEE, Washington DC, New York, 1996.

[26] M. A. Contreras, T. Nakada, A. O. Pudov, and R. Sites, "ZnO/ZnS (O, OH)/Cu (In, Ga)Se2/Mo solar cell with 18.6% efficiency," in *Proceedings of the Third World Conference of Photovoltaic Energy Conversion*, pp. 570–573, 2003.

[27] M. J. Jeng, Y. L. Lee, and L. B. Chang, "Temperature dependences of $In_xGa_{1-x}N$ multiple quantum well solar cells," *Journal of Physics D*, vol. 42, no. 10, p. 105101, 2009.

[28] G. O. Osayemwenre, E. L. Meyer, and S. Mamphweli, "An outdoor investigation of the absorption degradation of single-junction amorphous silicon photovoltaic module due to localized heat/hot spot formation," *Pramana*, vol. 86, no. 4, pp. 901–909, 2016.

[29] M. Z. Hussin, S. Shaari, A. M. Omar, and Z. M. Zain, "Amorphous silicon thin-film: behaviour of light-induced degradation," *Renewable and Sustainable Energy Reviews*, vol. 43, pp. 388–402, 2015.

[30] E. L. Meyer, "On the reliability, degradation and failure of photovoltaic modules," *Submitted in fulfilment of the requirements for the degree of Philosophiae doctor in the faculty of Science at the University of Port Elizabeth*, 2002.

[31] C. Y. Tsai and C. Y. Tsai, "Development of amorphous/-microcrystalline silicon tandem thin-film solar modules with low output voltage, high energy yield, low light-induced degradation, and high damp-heat reliability," *Journal of Nanomaterials*, vol. 2014, Article ID 861741, 10 pages, 2014.

[32] T. Yamawaki, S. Mizukami, A. Yamazaki, and H. Takahashi, "Thermal recovery effect on light-induced degradation of amorphous silicon solar module under the sunlight," *Solar Energy Materials & Solar Cells*, vol. 47, no. 1-4, pp. 125–134, 1997.

[33] D. E. Carlson and C. R. Wronski, "Amorphous silicon solar cell," *Applied Physics Letters*, vol. 28, no. 11, pp. 671–673, 1976.

[34] J. Sutterlueti, R. Kravets, M. Keller, H. Knauss, I. Sinicco, and A. Huegli, "Energy yield optimization and seasonal behaviour of micromorph thin film modules," in *25th European Photovoltaic Solar*, 2010.

[35] A. Virtuani, D. Pavanello, and G. Friesen, "Overview of temperature coefficients of different thin film photovoltaic technologies," in *25th European photovoltaic solar energy conference and exhibition/5th World conference on photovoltaic energy conversion*, pp. 6–10, September 2010.

[36] T. Shioda, "Delamination failures in longterm field-aged PV modules from point of view of encapsulant," in *Proceedings of the PV Module Reliability Workshop*, 2013.

[37] C. E. Chamberlin, M. A. Rocheleau, M. W. Marshall, A. M. Reis, N. T. Coleman, and P. A. Lehman, "Comparison of PV module performance before and after 11 and 20 years of field exposure," in *Proceedings of the 37th IEEE Photovoltaic Specialists Conference (PVSC '11)*, pp. 101–105, IEEE, Seattle, Wash, USA, 2011.

[38] E. E. Van Dyk and E. L. Meyer, "Analysis of the effect of parasitic resistances on the performance of photovoltaic modules," *Renewable Energy*, vol. 29, no. 3, pp. 333–344, 2004.

[39] E. L. Meyer and E. van Dyk, "Extraction of saturated current and ideality factor from measuring Voc and Isc of photovoltaic modules," *Submitted for Journal of Applied Physics*, 2002.

[40] J. Zaraket, M. Aillerie, and C. Salame, "Dark and illuminated characteristics of photovoltaic solar modules. Part I: Influence of dark electrical stress," in *AIP Conference Proceedings 1758*, 2016.

[41] H. D. Mohring, D. Stellbogen, R. Schäffler et al., "Outdoor performance of polycrystalline thin film PV modules in different European climates," in *Proceedings of the 19th European Photovoltaic Solar Energy Conference*, Paris, France, June 2004.

[42] P. M. Lundquist, "Characterization and simulation of the shading induced hot spot reliability problem in silicon photovoltaic solar modules," *a thesis submitted to the Graduate Faculty of the University of Colorado Springs in partial fulfilment of the requirements for the degree of Master of Science*, 2017, https://mountainscholar.org›handleLundquist_uccs_0892N_10244.

[43] G. Yang, R. A. C. M. M. van Swaaij, S. Dobrovolskiy, and M. Zeman, "Determination of defect density of state distribution of amorphous silicon solar cells by temperature derivative capacitance-frequency measurement," *Journal of Applied Physics*, vol. 115, no. 3, p. 034512, 2014.

[44] M. Stuckelberger, R. Biron, N. Wyrsch, F. J. Haug, and C. Ballif, "Review: progress in solar cells from hydrogenated amorphous silicon," *Renewable and Sustainable Energy Reviews*, vol. 76, pp. 1497–1523, 2017.

[45] N. Aste, G. Chiesa, and F. Verri, "Design, development and performance monitoring of a photovoltaic-thermal (PVT) air collector," *Renewable Energy*, vol. 33, no. 5, pp. 914–927, 2008.

[46] D. L. Staebler and C. R. Wronski, "Reversible conductivity changes in discharge-produced amorphous Si," *Applied Physics Letters*, vol. 31, no. 4, pp. 292–294, 1977.

[47] G. O. Osayemwenre, E. L. Meyer, R. T. Taziwa, and S. Mamphweli, "Photo-thermal degradation analysis of single-junction amorphous silicon solar module's EVA encapsulation," *Journal of Ovonic Research*, vol. 13, no. 4, pp. 225–232, 2017.

[48] A. Neftalí and C. Mendoza, *Influence of the p-type layer on the performance and stability of thin film silicon solar cells*, PhD thesis, 2017.

[49] C. Jiahao, "Evaluating thermal imaging for identification and characterization of solar cell defects," *thesis submitted for the partial fulfilment of the degree of master of Physics at Iowa State University*, Graduate Theses and Dissertations. 13973., 2014, https://lib.dr.iastate.edu/etd/13973.

[50] T. Wada, M. Kondo, and A. Matsuda, "Improvement of V_{oc} using carbon added microcrystalline Si p-layer in microcrystalline Si solar cells," *Solar Energy Materials and Solar Cells*, vol. 74, no. 1–4, pp. 533–538, 2002.

[51] R. D. Duke, S. Graham, M. Hankins et al., "Field performance evaluation of amorphous silicon (a-Si) photovoltaic systems in Kenya," *Methods and Measurements in Support of a Sustainable Commercial Solar Energy Industry*, 2000.

[52] S. Dubey, J. N. Sarvaiya, and B. Seshadri, "Temperature dependent photovoltaic (PV) efficiency and its effect on PV production in the world - a review," *Energy Procedia*, vol. 33, pp. 311–321, 2013.

[53] R. Singh, *Designing Amorphous Silicon Solar Cells for Optimal Photovoltaic Performance*, Charles Darwin University: CDU Library, 1st Ed. edition, 2009.

[54] N. M. Ravindra and V. K. Srivastava, "Temperature dependence of the maximum theoretical efficiency in solar cells," *Solar Cells*, vol. 80, no. 1, pp. 107–109, 1979.

[55] C. Cristofari, P. Poggi, G. Notton, and M. Muselli, "Thermal modelling of a photovoltaic module," in *Proceeding Sixth IASTED International Conference*, pp. 273–278, Gaborone, Botswana, 2006.

[56] M. G. Tamizh Mani, *Performance Losses and Reliability of Photovoltaic Modules*, International PV Reliability Workshop, Tempe, AZ, USA, 2009.

[57] D. D. Nguyen, *Modeling and reconfiguration of solar photovoltaic arrays under non-uniform shadow conditions*, PhD thesis submitted for the partial fulfilment for the aware of doctoral degree at Northeastern University, Boston, Massachusetts, 2008.

[58] A. Kołodziej, C. R. Wroński, P. Krewniak, and S. Nowak, "Silicon thin film multijunction solar cells," *Opto-Electronics Review*, vol. 8, no. 4, pp. 339–345, 2000.

[59] D. Nguyen and B. Lehman, "A reconfigurable solar photovoltaic array under shadow conditions," in *2008 Twenty-Third Annual IEEE Applied Power Electronics Conference and Exposition*, pp. 980–986, IEEE, February 2008.

[60] K. Kůsová, I. Pelant, and J. Valenta, "Nanocrystalline silicon for nanophotonics, bright trions in direct-bandgap silicon nanocrystals revealed by low-temperature single-nanocrystal spectroscopy," *Light: Science& Applications*, vol. 4, 2015.

[61] D. L. King, M. A. Quintana, J. A. Kratochvil, D. E. Ellibee, and B. R. Hansen, "Photovoltaic module performance and durability following long-term field exposure," *Progress in Photovoltaics: Research and Applications*, vol. 8, no. 2, pp. 241–256, 2000.

[62] A. V. Shah, H. Schade, M. Vanecek et al., "Thin-film silicon solar cell technology," *Progress in Photovoltaics: Research and Applications*, vol. 12, no. 23, pp. 113–142, 2004.

[63] S. M. M. Alpine, "Characterization and capture of photovoltaic system losses due to non uniform conditions," *PhD thesis submitted in partial fulfilment of the degree of philosophy of Engineering at Rice University*, 2013, https://scholarship.rice.edu/handle/1911/13110.

[64] F. Gao, D. Li, P. C. Loh, Y. Tang, and P. Wang, "Indirect dc-link voltage control of two-stage single-phase PV inverter," in *2009 IEEE energy conversion congress and exposition*, pp. 1166–1172, IEEE, September 2009.

[65] M. A. Green, K. Emery, D. L. King, Y. Hishikawa, and W. Warta, "Solar cell efficiency tables (version 29)," *Progress in Photovoltaics: Research and Applications*, vol. 15, 2007.

[66] E. L. Meyer, "Extraction of saturation current and ideality factor from measuring V_{oc} and I_{sc} of photovoltaic modules," *International Journal of Photoenergy*, vol. 2017, Article ID 8479487, 9 pages, 2017.

[67] E. van Dyk, E. L. Meyer, F. J. Vorster, and Leitch, "long term monitoring performance parameters," *Renewable Energy Journal*, vol. 34, pp. 302–312, 2004.

[68] J. Melskens, G. van Elzakker, Y. Li, and M. Zeman, "Analysis of hydrogenated amorphous silicon thin films and solar cells by means of Fourier transform photocurrent spectroscopy," *Thin Solid Films*, vol. 516, no. 20, pp. 6877–6881, 2008.

[69] A. I. Shkrebtii, Y. V. Kryuchenko, I. M. Kupchak et al., "Hydrogenated amorphous silicon (a-Si:H) based solar cell: material characterization and optimization," in *2008 33rd IEEE Photovoltaic Specialists Conference*, pp. 1–4, IEEE, May 2008.

[70] X. Deng and E. A. Schiff, "Amorphous silicon based solar cells," in *Handbook of Photovoltaic Science and Engineering*, pp. 505–565, John Wiley & Sons, Chichester, 2003.

[71] X. Deng and E. A. Schiff, *Handbook of Photovoltaic Science and Engineering, Amorphous Silicon based Solar Cells*, A. Luque and S. Hegedus, Eds., John Wiley & Sons, 2003.

[72] J. Sidawi, R. Habchi, N. Abboud et al., "The effect of reverse current on the dark properties of photovoltaic solar modules," *Energy Procedia*, vol. 6, pp. 743–749, 2011.

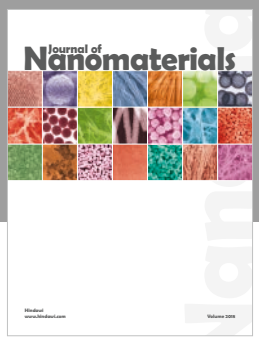

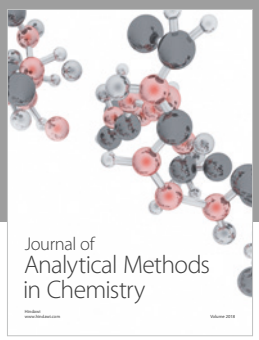

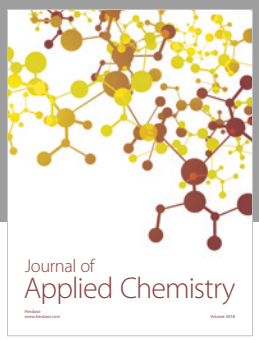

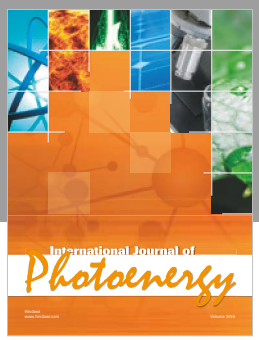

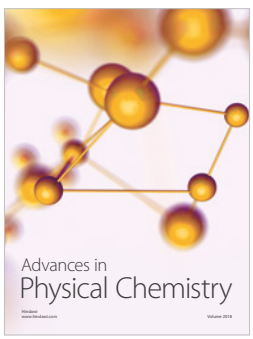

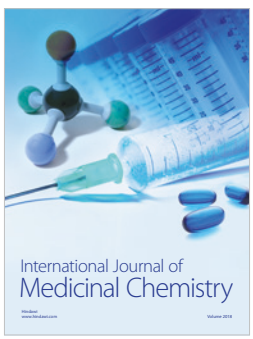

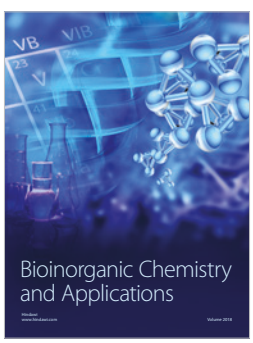

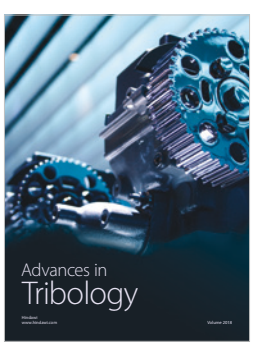

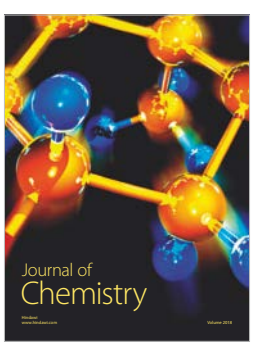

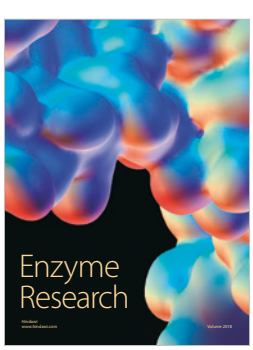

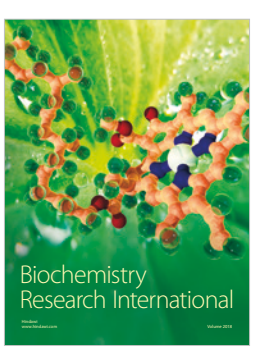

Hindawi

Submit your manuscripts at
www.hindawi.com